ONE-STEP HYDROTHERMAL SYNTHESIS OF FLUORESCENT CARBON DOTS AND Fe^{3+} DETECTION[**]

Kexin Yan, Jinlan Li, Yuansong Zheng, Zihong Yan*

College of Chemistry and Environmental Science at Kashgar University, Kashgar, China;
e-mail: yanzi0928@126.com

Carbon dots (CDs) are of great significance for metal ion detection. Herein, CDs without surface functional groups were synthesized through a simple one-step hydrothermal method using 4,4′-bipyridine as the carbon source. The results showed that the synthesized CDs have good selectivity for Fe^{3+} detection, and the CDs respond well to metal ions as Lewis bases. This detection method is unlikely to be affected by sewage systems because it has excellent sensitivity. The detection range for Fe^{3+} concentrations is between 1.0×10^{-8} and 1.0×10^{2} mol/L, and the detection limit is 1.0×10^{-8} mol/L.

Keywords: *carbon dots, fluorescent, Fe^{3+} detection.*

ОДНОСТАДИЙНЫЙ ГИДРОТЕРМАЛЬНЫЙ СИНТЕЗ ФЛУОРЕСЦЕНТНЫХ УГЛЕРОДНЫХ ТОЧЕК ДЛЯ ОБНАРУЖЕНИЯ Fe^{3+}

K. Yan, J. Li, Y. Zheng, Z. Yan*

УДК 535.37:546.26:546.72

Колледж химии и наук об окружающей среде Кашгарского университета, Кашгар, Китай;
e-mail: yanzi0928@126.com

(Поступила 21 июня 2022)

Углеродные точки (CDs) без поверхностных функциональных групп синтезированы простым одностадийным гидротермальным методом с использованием 4,4′-бипиридина в качестве источника углерода. Показано, что синтезированные CDs обладают хорошей селективностью к обнаружению Fe^{3+} и реагируют на ионы металлов как основания Льюиса. Диапазон обнаружения концентраций Fe^{3+} от 1.0×10^{-8} до 1.0×10^{2} моль/л, предел обнаружения 1.0×10^{-8} моль/л.

Ключевые слова: *углеродные точки, флуоресценция, обнаружение Fe^{3+}.*

Introduction. Carbon dots (CDs), a new type of carbon nanomaterial with sizes less than 10 nm, can emit blue-green fluorescence [1]. Currently, carbon dots offer fast responses, good selectivity, high sensitivity, and superior reproducibility and stability; thus, carbon dot fluorescent techniques are widely used for detection in diverse samples [2–4]. According to the different internal structures of carbon dots, they can be divided into the following three categories: graphene quantum dots (GQDs), carbon nanodots and polymer dots (PDs). GQDs and CDs are most widely used in current research environments and are defined as ultrafine carbon material fragments with adjustable degrees of carbonization, and their surfaces contain a large number of functional groups [5, 6]. At present, luminescent carbon nanodots can be prepared on a large scale in a variety of ways [7]. Although the preparation processes are different, most CDs show blue or green luminescence [8].

Fluorescent CDs have remarkable properties. Their excitation spectrum is wide, and their emission spectrum is redshifted with increasing excitation wavelength [9, 10]. Most syntheses of CDs are completed by one-step processes, a wide range of raw materials and simple processes are available, and the methods are

[**] Full text is published in JAS V. 90, No. 3 (http://springer.com/journal/10812) and in electronic version of ZhPS V. 90, No. 3 (http://www.elibrary.ru/title_about.asp?id=7318; sales@elibrary.ru).

suitable for producing large number of CDs. With increasing research in CDs, the field has expanded and includes metal ion detection, chemical sensors, biological probes, and photocatalysis [11–16]. CDs are not only synthesized from different raw materials because of the availability of simple, green and effective synthesis routes, but also because these biological macromolecules have good biocompatibility and excellent water stability, which has aroused great interest [17, 18]. These biomolecules are rich in amino and carboxyl groups that can promote water stability and surface binding in CDs, and these properties are relevant for a variety of biological applications [19].

Heavy metal ions have harmful effects on human health and the environment, and Fe^{3+} is a metal ion that is very important to biological systems and environmental processes and can coordinate with a variety of regulatory proteins in biological systems. It is also a ubiquitous metal in biochemical processes such as cell metabolism, electron transport, enzyme catalysis, oxygen transport and DNA and RNA synthesis [20–22]. The presence of too much or too little iron ion can cause physical diseases, such as anemia, mental decline, arthritis, diabetes and cancer [23, 24]. In addition, the Fe^{3+} ion concentration is an important sign of Parkinson's disease, and excess Fe^{3+} ions can lead to cytotoxicity. Furthermore, Fe^{3+} is an important species for environmental monitoring; therefore, an accurate and rapid method for detecting Fe^{3+} in biological systems and in the natural environment is very important [25]. CDs are widely used as fluorescent probes for the detection of metal ions, with good selectivity and sensitivity [26, 27].

In this study, CDs are synthesized by a hydrothermal method using 4-bipyridine as a precursor, and the specific fluorescence detection of Fe^{3+} is realized. The morphology, structure, and fluorescence properties of the CDs are characterized by scanning electron microscopy (SEM) and fluorescence spectrophotometry. The effects of reaction concentration, solvent, temperature, and time on the luminescence properties of CDs are studied. The fluorescence quenching property of CDs is used to realize the specific detection of Fe^{3+}.

Experimental. 4,4′-Bipyridine was purchased from Aladdin. All other reagents were of analytical grade and were used as purchased without further purification. Deionized water was used in all experiments. Fluorescence experiments were performed on a PerkinElmer LS55 fluorescence spectrometer. Scanning electron microscopy (SEM) analyses were conducted with a JSM-7800F instrument.

The CDs were synthesized by a one-step hydrothermal method. 4,4′-bipyridine was first dispersed ultrasonically in 10 mL of ethanol for 30 min, and then the obtained mixture was sealed in a 25-mL Teflon-lined stainless-steel kettle and subjected to heating. After the reaction, the solution of CDs was cooled to room temperature. The resultant yellowish liquid was dialyzed against water using dialysis membranes (retained molecular weight: 1000 Da) for 48 h to remove impurities. Finally, CDs were obtained by heating the dialysate.

We used 4,4′-bipyridine (*Mw* = 156.18) as the raw material for the reaction. The experimental conditions for preparing the CDs were optimized, and the CDs produced using the optimal conditions were tested by changing their concentration, solvent, reaction time and temperature. The fluorescence intensity of CDs under different conditions was tested by a fluorescence spectrophotometer. The test revealed the optimal reaction condition: 0.3 mmol of reactant at 200°C reacted in a reactor with ethanol and deionized water (1:1) as solvents for 8 h.

The detection of metal ions was carried out on a fluorescence spectrophotometer. Metal salt solutions of the same concentration (Ag^{+}, Bi^{3+}, Cd^{2+}, Co^{2+}, Ga^{3+}, Fe^{3+}, Hg^{+}, K^{+}, Mg^{2+}, Mn^{2+}, Na^{+}, Ni^{2+}, Pb^{2+}, Sn^{2+}, and Yb^{3+}) were prepared in deionized water. In the experiment, 1 mL of CDs was dispersed in 1 mL of deionized water. The best quenching effect of Fe^{3+} was obtained during fluorescence quenching. By testing different levels of Fe^{3+}, the optimal quenching of CD fluorescence by Fe^{3+} was determined.

Results and discussion. *Characterization of CDs.* After drying the prepared carbon dots, we were able to visualize their morphology, as shown in Fig. 1a. The CDs consisting of light-yellow needle-like powders on the outer gauge were in a granular state. The morphology of the CDs was characterized by high-resolution transmission electron microscopy (HRTEM). Under a scanning electron microscope, the CDs were composed of these small aggregated particles. The shape of the sample observed at 100 nm is shown in Figs. 1b,c. These nanoparticles were 15–30 nm in size and were evenly distributed. The shape of the sample observed at 1 μm is shown in Fig. 1d. Its surface had an uneven particle distribution.

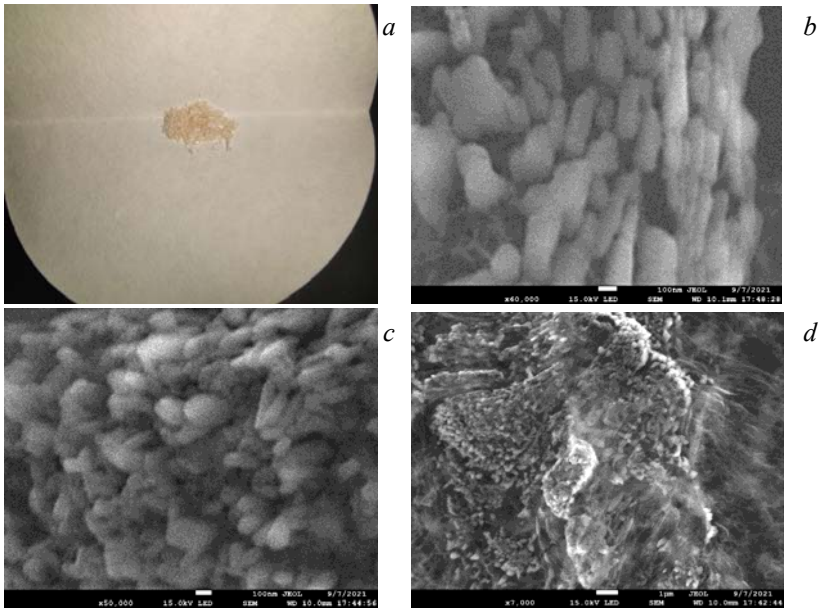

Fig. 1. (a) Shape of the sample in the ordinary state; (b) and (c) shape of the sample observed at 100 nm; (d) shape of the sample observed at 1 μm.

We tested the optimal fluorescence intensity of the CDs under different excited states (220–420 nm), a single frequency peak appears at 320 nm on the abscissa, and a multiple frequency peak appears at 640 nm. These interference peaks are discarded to obtain the best absorption peak at 413 nm. When the excitation wavelength of the CDs was 330 nm, the emission wavelength of the CDs was 413 nm (the fluorescence intensities of the CDs tested later are based on this standard). At the same time, it can be seen from Fig. 2a that the fluorescence at 340 nm and beyond appeared to redshift. To determine the durability of the CDs, we tested the intensity of the CDs immediately after they were removed from the reactor and compared it with their fluorescence intensity after 2 months at room temperature. The results show that with time, the fluorescence intensity decreased significantly under an excitation wave of 330 nm, as shown in Fig. 2b.

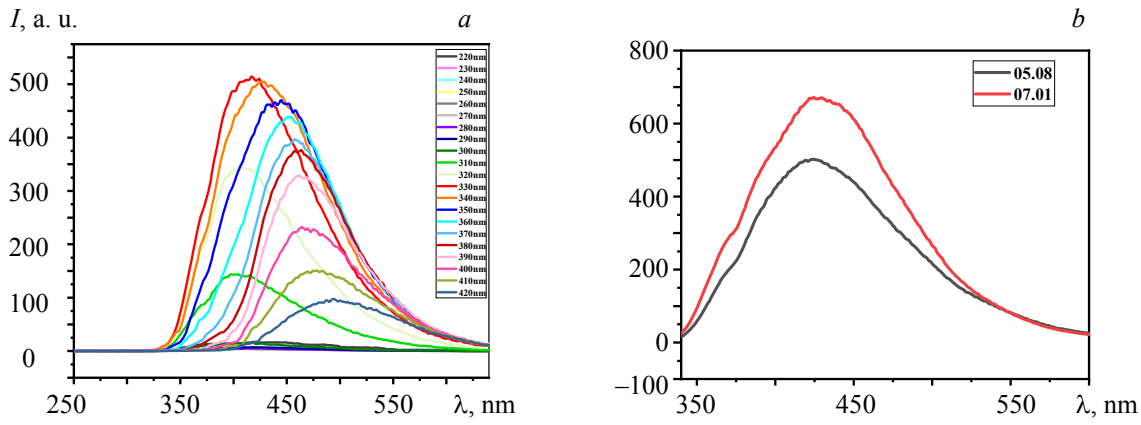

Fig. 2. (a) Excitation spectra and emission slope spectra of fluorescence; (b) Change in the fluorescence intensity of the carbon dots after 2 months.

The fluorescence quantum yield (Φ) is an important luminescence parameter for fluorescent substances and is defined as the number of fluorescent photons emitted by fluorescent substances after light absorption. The calculation of the Φ value usually involves the use of a reference method. The larger the Φ value is, the stronger the fluorescence intensity, but by definition, the value is generally less than 1. By comparing the integrated emission spectrum and absorbance of the fluorescent substance to be tested with that of a substance

with known fluorescent quantum yield under the same assay conditions, the fluorescence quantum yield formula can be expressed as:

$$\Phi = I/I_R \times A_R/A \times \eta/\eta_R \times \Phi_R,$$

where I is the integral area of the emission spectrum, A is the ultraviolet–visible absorbance at the fluorescence excitation wavelength, and η is the refractive index of the solvent (the solvent of the sample and the reference is the same, so the refractive index is the same: 1.334). The quantum yield at the maximum excitation wavelength of 330 nm is 0.116.

Quenching by metal ions. The prepared CDs were used to quench different metal ions (Ag^+, Bi^{3+}, Cd^{2+}, Co^{2+}, Ga^{3+}, Fe^{3+}, Hg^+, K^+, Mg^{2+}, Mn^{2+}, Na^+, Ni^{2+}, Pb^{2+}, Sn^{2+}, and Yb^{3+}). Under an excitation wavelength of 330 nm, the CDs were quenched by different metal ions, resulting in a decrease in fluorescence intensity, as shown in Fig. 3a. As expected, the quenching effect of the metal ion Fe^{3+} was better determined by changing the intensity of fluorescence. The synthesized CDs have the best fluorescence quenching effect for Fe^{3+}, which precisely reflected the selectivity of 4,4′-bipyridine for Fe^{3+}. Figure 3b shows a histogram of CD quenching intensities with different ions, and it allows us to observe the selectivity of the CDs for Fe^{3+} more intuitively.

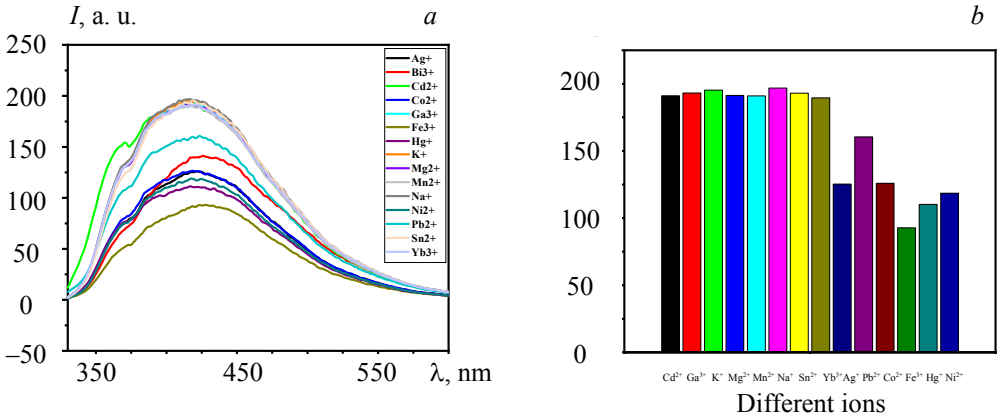

Fig. 3. (a) Fluorescence intensity of CDs quenched by different metal ions at 1 mmol/L; (b) Fluorescence intensity at carbon dots quenched by 1 mmol/L metal ions.

Under irradiation with a 365-nm UV lamp, the aqueous solution appeared blue-green in a dark box. Compared with the original solution, the blue-green fluorescence was significantly enhanced, which was due to the aggregation of 4,4′-bipyridine at high temperatures and pressures, which greatly increased the originally weak fluorescence intensity to a strong blue-green fluorescence. The concentrations of the aqueous solutions that quenched the CDs are as follows (mmol/L): 100, 75, 50, 10, 5, 1, 0.5, 0.1, 0.05, 0.01, 0.005, 0.001, 0.0001.

Under an excitation wavelength of 330 nm, CD quenching by Fe^{3+} ions was analyzed in detail. In the concentration range of 0.1 μmol/L–100 mmol/L, as shown in Fig. 4a, the sensitivity of CDs to Fe^{3+} ions was very high. Fe^{3+} (0.1 μmol/L) could be detected by 1 mL of CD solution, and the lower limit of detection was 0.1 μmol/L Fe^{3+}. For concentrations of Fe^{3+} between 0.1 and 1 mmol/L, the fluorescence intensity showed an excellent linear relationship, as shown in Figs. 4b,c. Surprisingly, Fe^{3+} had little effect on the quenching of CDs in buffer solutions at different pH values, as shown in Fig. 4d, and the fluorescence intensity was essentially unchanged. In short, in general sewage systems (other than those in strong acid and base systems), pH is likely to have little effect on CDs. To determine the effect of ion interference, Fe^{3+} was mixed with different ions, as shown in Fig. 4e. The presence of different ions had little effect on the Fe^{3+} quenching of CDs, which further demonstrated the selectivity of the CD solution to Fe^{3+}.

CD fluorescence quenching mechanism of Fe^{3+}. The molecular formula for 4,4′-bipyridine is $C_{10}H_8N_2$, and its network topological structures are formed by the orbital delocalization of rings, by π orbital interactions, and by polymerization and crosslinking. The highly crosslinked structure limits vibration and rotation, making nonradiative transitions difficult and increasing fluorescence intensity. It contains nitrogen, and the nitrogen content accounts for 17.93% of its elemental content. It is a rigid, linear, double-base ligand that contains no branched chains and has low steric resistance. The nitrogen atoms at both ends can simultane-

ously coordinate with different metal atoms. The unshared electron pairs on the nitrogen atoms can accept protons, showing alkalinity and acting as weak Lewis bases. The fluorescence quenching of CDs can be clearly seen in the fluorescence spectrogram when Fe^{3+} ions coordinate with the Lewis base.

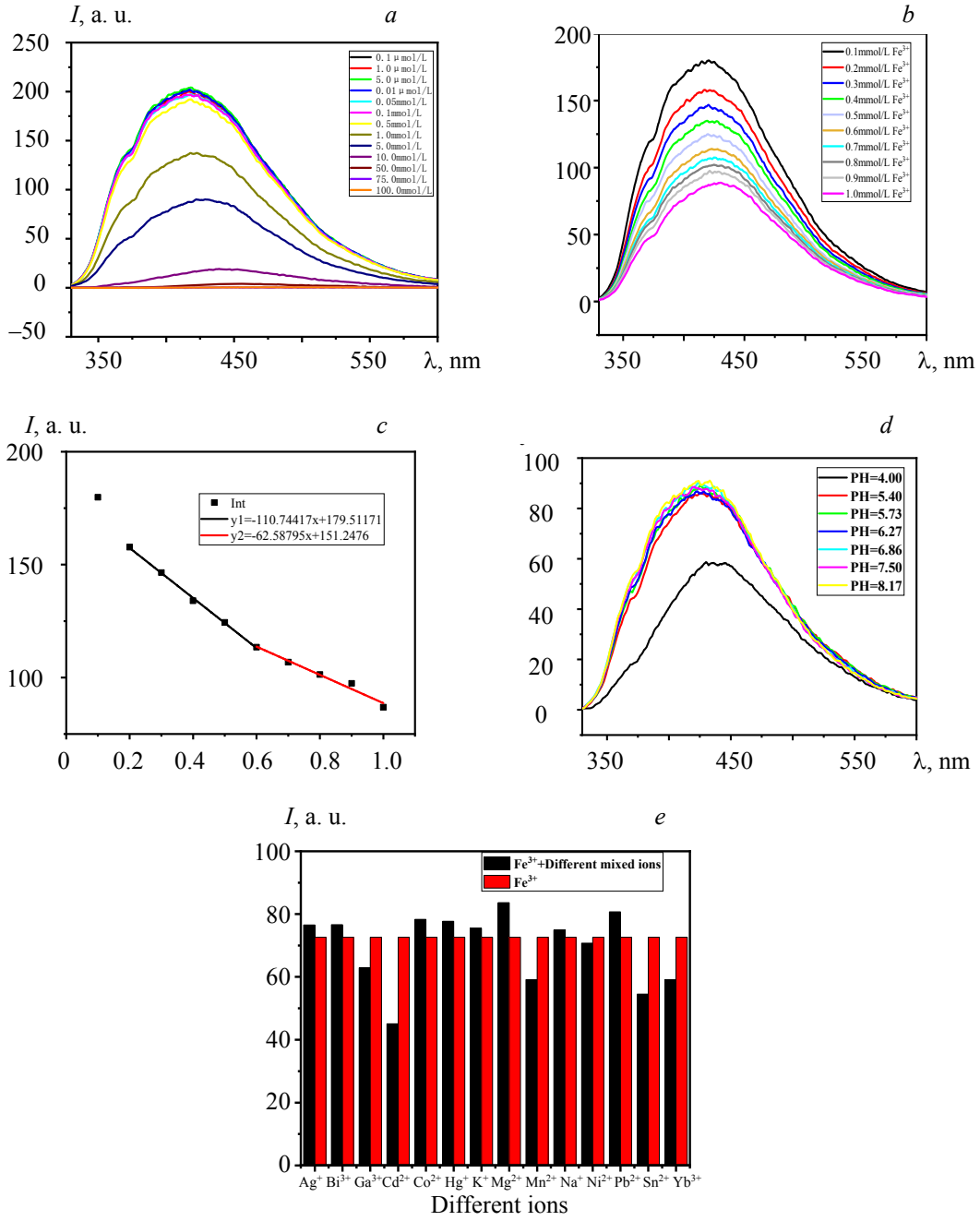

Fig. 4. (a) Fluorescence of CDs quenched by Fe^{3+} at different concentrations; (b) Fluorescence of CDs quenched by Fe^{3+} at 0.1–1 mmol/L; (c) Linear relationship between CDs quenched by Fe^{3+} at 0.1–1 mmol/L; (d) Fluorescence intensity of CDs at different pH values; (e) Effect of interfering ions on fluorescence.

Conclusions. Carbon dots without surface functional groups are prepared by a simple one-step hydrothermal method using 4,4′-bipyridine. The product can emit visible blue-green light under ultraviolet light irradiation, and the optimal excitation wavelength is 330 nm. The carbon dots act as special Lewis bases in response to metal ions. This study reveals that the quenching effect of Fe^{3+} on carbon dots is very apparent,

with a good linear relationship between 0.1 and 1 mmol/L. The detection limit is 1×10^{-8}, and this is not likely to be affected by general sewage systems. The quantum dots are easy to synthesize, have excellent performance and can be used for the detection of Fe^{3+} in actual samples. They play important roles in the preparation of carbon dots and in the rapid and sensitive detection of metal ions.

This research was supported by the Natural Science Foundation of Xinjiang Uygur Autonomous Region (No. 2022D01A018).

REFERENCES

1. P. Yu, X. Wen, Y.-R. Toh, J. Tang, *J. Phys. Chem. C*, **116**, No. 48, 25552–25557 (2012).
2. S.-T. Yang, X. Wang, H. Wang, F. Lu, P. G. Luo, L. Cao, M. J. Meziani, J.-H. Liu, Y. Liu, M. Chen, Y. Huang, Y.-P. Sun, *J. Phys. Chem. C*, **113**, No. 42, 18110–18114 (2009).
3. C. Hu, M. Li, J. Qiu, Y.-P. Sun, *Chem. Soc. Rev.*, **48**, No. 8, 2315–2337 (2019).
4. P. Miao, K. Han, Y. Tang, B. Wang, T. Lin, W. Cheng, *Nanoscale*, **7**, No. 5, 1586–1595 (2015).
5. S. N. Baker, G. A. Baker, *Angew. Chem. Int. Ed.*, **49**, No. 38, 6726–6744 (2010).
6. Y.-P. Sun, B. Zhou, Y. Lin, W. Wang, K. A. S. Fernando, P. Pathak, M. J. Meziani, B. A. Harruff, X. Wang, H. Wang, P. G. Luo, H. Yang, M. E. Kose, B. Chen, L. M. Veca, S.-Y. Xie, *J. Am. Chem. Soc.*, **128**, No. 24, 7756–7757 (2006).
7. P. Miao, K. Han, Y. Tang, B. Wang, T. Lin, W. Cheng, *Nanoscale*, **7**, No. 5, 1586–1595 (2015).
8. L. Wang, S.-J. Zhu, H.-Y. Wang, S.-N. Qu, Y.-L. Zhang, J.-H. Zhang, Q.-D. Chen, H.-L. Xu, W. Han, B. Yang, H.-B. Sun, *ACS Nano*, **8**, No. 3, 2541–2547 (2014).
9. Y. Liu, In: *Multifunctional Nanoprobes*, Springer Theses, Springer Singapore, Singapore, 51–64 (2018).
10. T.-Y. Wang, C.-Y. Chen, C.-M. Wang, Y. Z. Tan, W.-S. Liao, *ACS Sens.*, **2**, No. 3, 354–363 (2017).
11. Z. Ye, G. Li, J. Lei, M. Liu, Y. Jin, B. Li, *ACS Appl. Bio Mater.*, **3**, No. 10, 7095–7102 (2020).
12. S. Huang, J. Yao, X. Chu, Y. Liu, Q. Xiao, Y. Zhang, *J. Agric. Food Chem.*, **67**, No. 40, 11244–11255 (2019).
13. D. Hong, X. Deng, J. Liang, J. Li, Y. Tao, K. Tan, *Microchem. J.*, **151**, 104217 (2019).
14. W. Li, S. Wang, Y. Li, et al. *Carbohydr. Polym.*, **175**, 7—17 (2017).
15. Y. Chen, Q. Yang, P. Xu, L. Sun, D. Sun, K. Zhuo, *ACS Omega*, 9 (**2017)**.
16. F. Wang, S. Pang, L. Wang, Q. Li, M. Kreiter, C. Liu, *Chem. Mater.*, **22**, No. 16, 4528–4530 (2010).
17. D. Chen, X. Chen, H. Gao, J. Zhong, *RSC Adv.*, **8**, No. 52, 29855–29861 (2018).
18. J. Ge, Q. Jia, W. Liu, L. Guo, Q. Liu, M. Lan, H. Zhang, X. Meng, P. Wang, *Adv. Mater.*, **27**, No. 28, 4169–4177 (2015).
19. Z. Zhang, J. Hao, J. Zhang, B. Zhang, *RSC Adv.*, **2**, No. 23, 8599 (2012).
20. L. Li, Y.-F. Han, Z.-B. Zheng, C.-A. Wang, K. Nie, J.-K. Li, R.-F. Zhang, J. Ru, C.-L. Ma, *J. Solid State Chem.*, **295**, 121887 (2021).
21. X. Zhu, Z. Zhang, Z. Xue, C. Huang, Y. Shan, C. Liu, X. Qin, W. Yang, X. Chen, T. Wang, *Anal. Chem.*, **89**, No. 22, 12054–12058 (2017).
22. M. S. Petronek, D. R. Spitz, G. R. Buettner, B. G. Allen, *Cancers*, **11**, No. 8, 1077 (2019).
23. Y. Du, B. J. Lim, B. Li, Y. S. Jiang, J. L. Sessler, A. D. Ellington, *Anal. Chem.*, **86**, No. 15, 8010–8016 (2014).
24. J. F. Zhang, Y. Zhou, J. Yoon, J. S. Kim, *Chem. Soc. Rev.*, **40**, No. 7, 3416 (2011).
25. W.-W. Xiong, G.-H. Yang, X.-C. Wu, J.-J. Zhu, *ACS Appl. Mater. Interfaces*, **5**, No. 16, 8210–8216 (2013).
26. N. Kohli, O. Singh, R. C. Singh, *Appl. Phys. A*, **109**, No. 3, 585–590 (2012).
27. X. Wu, C. Ma, J. Liu, Y. Liu, S. Luo, M. Xu, P. Wu, W. Li, S. Liu, *ACS Sus. Chem. Eng.*, **7**, No. 23, 18801–18809 (2019).